The Subsonic Near-Wake of an Axisymmetric Semielliptical Afterbody

R. A. Merz*
Lafayette College, Easton, Pennsylvania
C. H. Yi†
Union Carbide Corporation, Bound Brook, New Jersey
and
C. E. G. Przirembel‡
Clemson University, Clemson, South Carolina

The near-wake of axisymmetric semielliptical afterbody was studied experimentally in a wind tunnel at 47 m/s using an upstream support system to minimize disturbances to the wake. The flowfield was surveyed with a variety of pressure and hot-wire probes. This paper presents the mean flowfield characteristics for the entire near-wake region. The results include static and stagnation pressure distributions as well as velocity profiles. Separation occurred at 0.38 model radii upstream of the base, while realignment was found at 0.2 model radii downstream. Centerline velocity recovery is slower than for blunt bases, but far-wake similarity was found as early as 0.4 radii downstream. The overall flowfield is heavily influenced by the wall geometry. The data presented will serve as a quantitative basis for the development and evaluation of analytical solutions.

Nomenclature

C_p = pressure coefficient [Eq. (1)]
D = model diameter
P = pressure
R = model radius, 31.12 mm
r = local radius of model
V = velocity
V_d = velocity defect
X = axial distance from base (positive = downstream, negative = upstream)
Y = radial distance from centerline
Y_b = location where $V_d = \frac{1}{2} V_{d_{max}}$
β = wall angle
ρ = density
ϕ = angular coordinate (see Fig. 3)

Subscripts

max = maximum
∞ = freestream condition
0 = stagnation condition

Introduction

BOUNDARY-layer separation from a body moving through a real fluid is usually due to an abrupt change in surface geometry or a sufficiently strong adverse pressure gradient. Such adverse pressure gradients may be caused by wall curvature. Both types of flow separation may be found on vehicles such as cars, trucks, trains, planes, and other high-speed transportation systems. At the rear of these vehicles, where separation is most likely to occur, the free shear layers that are formed pass on downstream to form the wake of the vehicle. The flow separation and subsequent wake greatly influence the drag and stability of a vehicle.

Numerous investigators have studied boundary-layer separation for many years and comprehensive reviews of the classical references may be found in Refs. 1 and 2. Much of the work for incompressible flows has been directed at two-dimensional geometries as opposed to axisymmetric and three-dimensional flows. Recent studies by Yi and Przirembel[3] and Presz and Pitkin[4,5] have dealt with separation from axisymmetric, curved afterbodies. These studies have concentrated on the boundary layer, its properties, the separation process, and the criteria for separation. While the boundary layer has been studied extensively, there appears to be a paucity of information available on the near-wake behind curved afterbodies. In light of this apparent need, a comprehensive experimental investigation of the near-wake of a curved afterbody was conducted. The data obtained represent the most extensive information available on this flowfield and will serve as a basis for the development and evaluation of analytical solutions.

In order to investigate the fundamental structure of an axisymmetric near-wake, a simple curved afterbody was selected. Specifically, the ellipsoidal afterbody Yi and Przirembel[3] had used in their study was chosen because of the abundance of information available on the boundary layer and its separation. Figure 1 shows a schematic of the important flowfield components. The attached boundary layer continues to grow as the mean pressure increases and the velocity decreases. Finally, the flow separates near the trailing edge of the body forming a small recirculation region. The free shear layer is realigned with the mainstream and then accelerates rapidly. Further downstream the far-wake with its familiar similarity profile is established and the mean velocity recovery continues with the centerline turbulence decaying slowly.

Experiment

This experiment was conducted in the Rutgers Low-Turbulence Subsonic Wind Tunnel. It is an open-circuit induction facility with a closed test section (30.5 × 45.7 cm). A cylindrical forebody 1.52 m long and 6.22 cm in diameter was suspended on the tunnel centerline by two sets of 0.13

Received July 31, 1984; revision received Dec. 1, 1984.

*Assistant Professor, Mechanical Engineering Department. Member AIAA.
†R&D Manager, Polyolefins Division.
‡Professor and Head, Mechanical Engineering Department. Associate Fellow AIAA.

mm thick bronze straps. These straps and the forebody suspension system were located in the tunnel plenum chamber where the velocity was less than 2.75 m/s. Figure 2 shows a schematic of the tunnel and the experimental setup.

A semielliptical body of revolution with an axis ratio of 4:1 was attached to the end of the cylindrical model in the test section. The model and coordinate system used throughout this paper are shown in Fig. 3. Most of the measurements were made in one plane; namely, the plane containing the x axis and $\phi = 0$.

The model had nine pressure orifices along the curved surface. The holes were 45 deg apart around the model to ensure minimum interference with each other. Alignment of the model was aided by four shoulder pressure taps spaced 90 deg apart around the circumference of the model at an axial location 3.18 mm upstream from the start of the wall curvature. Equal readings from these taps indicated that the model was aligned with the freestream and that the flow was axisymmetric. All pressure taps were 0.56 mm in diameter and drilled normal to the surface of the model. The surface pressures were monitored throughout the test program to ensure that the flow over the model matched that of Yi and Przirembel,[3] and to make sure that no changes occurred while the wake was being surveyed.

To ensure the presence of a fully developed turbulent boundary layer, a ring-shaped trip with a 0.79 mm high triangular cross section was mounted 10 model radii upstream from the base of the model. This device successfully induced fully developed turbulent flow and also thickened the boundary layer so that the axisymmetric effect would be enhanced.

The near wake was surveyed with a wide variety of pressure and hot-wire probes. Except for the tips of these probes, the entire measurement system was located outside of the test section. A traversing mechanism allowed the probe position to be determined to within ± 0.013 mm.

A 1.59 mm diam Kiel probe was used to measure stagnation pressure in the near wake where it was difficult to determine flow angularity and, thus, properly align standard pitot probes. A disk probe was used to determine the static pressures in the flowfield. The probe consisted of a sharp-edged flat disk (1.52 mm in diameter, 0.76 mm thick) attached to the end of a tube (3.18 mm o.d., 2.46 mm i.d.). A pressure orifice located at the center of one side of the disk sensed the static pressure. While it was very sensitive to pitch angle (i.e., the angle of attack of the disk plane), the disk probe had virtually no directional sensitivity in the radial direction and, therefore, is quite suitable for measurements in the shear layer. Further details regarding disk probes may be found in Ref. 6. The probe was aligned in the freestream to give the same static pressure as a conventional static pressure probe. It was then moved in toward the tunnel centerline through the shear layer without changing the pitch angle. The static and stagnation pressures on the centerline of the recirculation region were measured by extending a straight pitot-static tube out from the tip of the model base. Since the flow in this region is toward the model, the tip of the probe measured the stagnation pressure while the taps on the side of the probe sensed the static pressure. All pressures were read on a Zeiss variable-inclination cistern-type alcohol manometer with a least count of 0.05 mm of water.

Many types of hot-wire probes were used to measure the velocities in the shear layer. For the major portion of this study, 55F11 straight probes and 55F14 boundary-layer probes from DISA's "Golden Line" series were chosen. Due to their unique geometrical arrangement, these probes are particularly free from support prong disturbances and are insensitive to yaw angle changes. The signal from the hot-wire probe was processed by a DISA solid-state constant-temperature universal anemometry system (55D00) with a signal linearizer (55D10). Only the mean velocities determined from the hot-wire measurements are presented in this paper. Information on the turbulence in the flowfield will be presented in a second paper at a later date.

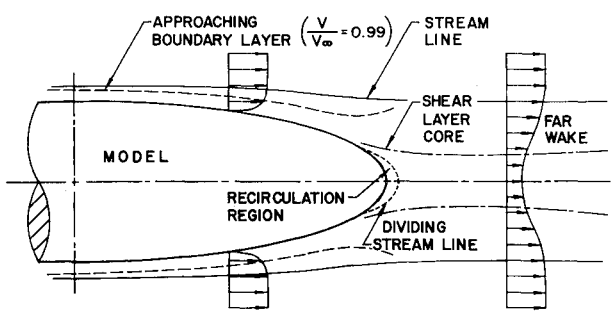

Fig. 1 Schematic of flowfield.

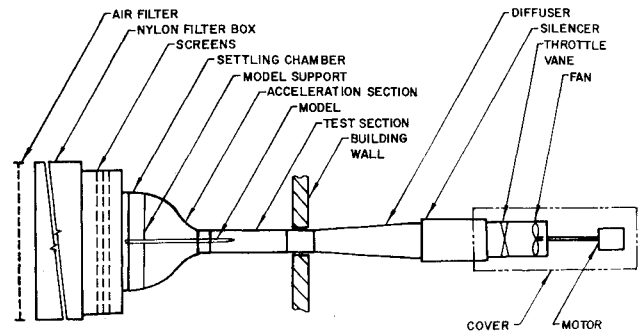

Fig. 2 Wind tunnel.

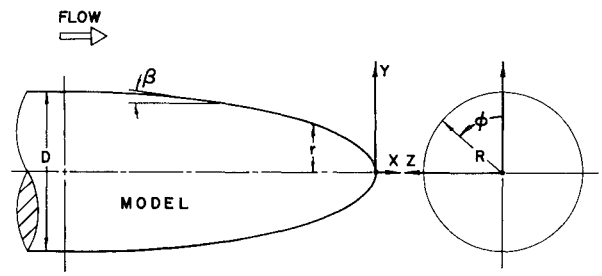

Fig. 3 Coordinate system.

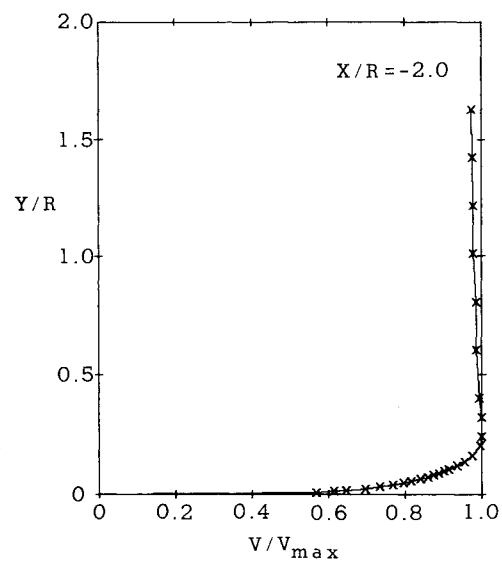

Fig. 4 Typical boundary-layer profile.

Finally, throughout the course of this investigation various flow visualization techniques were employed for qualitative observations. The techniques used included surface-oil film, smoke injection from the tunnel inlet, dyed water injection through the pressure taps, and tuft "tell-tale" traversing of the regions of interest.

The tests were conducted at a freestream velocity of 47.25 m/s with a corresponding Reynolds number of 3.08×10^6/m and a Mach number of 0.14. The stagnation pressure at the entrance to the contraction was just below atmospheric pressure, while the stagnation temperature was 295 K $\pm$ 3.3 K. The test section had a static pressure of -1.38 kPa gage and a freestream turbulence intensity of 0.2%. Measurements prior to the installation of the centerbody showed no measurable axial static pressure gradient in the test section. This is due to a very slight divergence of the test section walls in the axial direction. The boundary layer on the centerbody was turbulent, fully developed, and could be adequately described by a 1/7 power law profile. Figure 4 shows a typical boundary-layer profile. Further details on the boundary layer may be found in Ref. 3.

Results

The measured pressures, static and stagnation, were reduced to pressure coefficient form:

$$C_p=\frac{P-P_\infty}{\frac{1}{2}\rho_\infty V_\infty^2}=\frac{P-P_\infty}{P_{0_\infty}-P_\infty} \tag{1}$$

where the freestream static and dynamic pressures were measured at an axial location 7 model radii upstream of the base and 0.633 radii away from the model surface. This is the same location Yi and Przirembel[3] used for their reference location. They have shown that this point is outside the region of influence of the base flowfield and is representative of the freestream and, thus, a good choice for a reference condition. It should be noted that the absolute values of the pressure coefficients vary significantly depending on the choice of the reference condition. However, it is their relative values and characteristics that are of primary importance in understanding the flowfield.

The variation of static and stagnation pressure coefficients along the surface of the afterbody is plotted in Fig. 5. The static pressures were obtained by surface pressure taps, while the stagnation values were obtained from a boundary-layer probe resting on the model's surface.

The static pressure goes through a favorable-adverse gradient process and finally crosses over the stagnation pressure coefficient which has been decreasing almost linearly. This crossover point is located at $X/R=-0.32$ and represents the apparent separation line. Other techniques, such as oil flow, water injection, and the "tell-tale" traverse, indicated a time-averaged separation point between $X/R=-0.35$ and -0.40. The discrepancy is caused by the finite probe size. Although some unsteadiness in the location of the separation line was observed, no periodic fluctuations were detected by any of the above techniques.

By considering the error characteristics of the various techniques employed for the determination of the separation line, including flow visualization, the most probable value was estimated to be $X/R=-0.38$, corresponding to a wall angle of 27 to 29 deg. It is interesting to note that Nice et al.[7] observed separation at a similar wall angle for a two-dimensional curved backstep.

Figure 5 shows the stagnation and static pressure variation along the centerline. Up to the realignment point located at $X/R=0.2$, the two pressures are almost identical. The stagnation pressure starts to increase rapidly in the near-wake region. At first, the static pressure increases slightly with the stagnation pressure, similar to a blunt base as observed by Merz et al.[8] and McErlean and Przirembel.[9] However, it soon drops quickly and asymptotically approaches the freestream pressure as the centerline velocity is recovered and the velocity profile gets flatter.

The base pressure coefficient was observed to be 0.168 at the tip of the base. Merz et al.,[8] McErlean and Przirembel,[9] Van Wagnen,[10] and Przirembel and Riddle[11] reported base pressure coefficients of -0.11, -0.165, -0.12, and -0.125, respectively, for a blunt base model. For an ellipsoidal model, however, Chevray's[12] measurement showed the base pressure coefficient to be 0.158, which is in good agreement with the present results. As mentioned earlier, the positive base pressure coefficient resulted from the fact that the pressure recovery before the separation process was much larger than the loss after the separation.

The realignment or rear stagnation point was difficult to determine due to the highly unstable nature of the recompression region. At this point, it should be remembered that for this type of highly turbulent flow, a "point" of separation or realignment is rather a hypothetical term, which is defined for convenience, and "region" would be a more realistic term. From the pressure measurements as well as the flow visualization methods, the realignment was observed to occur around $X/R=0.2$, which is identical to the value obtained by Chevray.[12]

The velocity variation along the centerline is plotted as a solid line in Fig. 6. The reversed flow in the recirculation region is insignificant for the elongated afterbodies. Up to about $X/R=2.0$, the recovery of the velocity is fairly rapid, but soon levels out and increases very slowly. Chevray's[12]

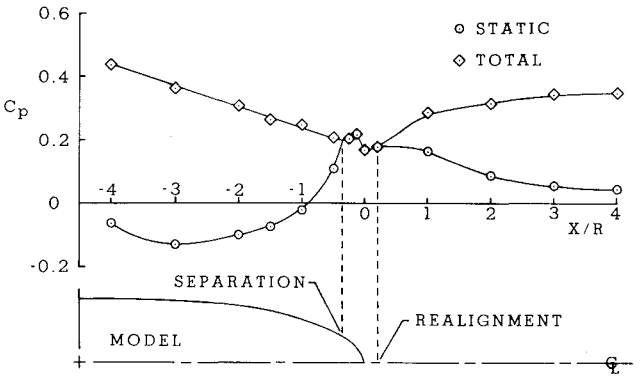

Fig. 5 Surface and centerline pressures.

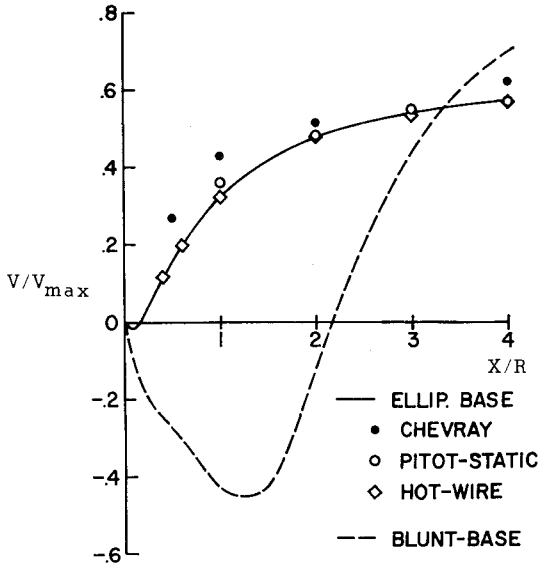

Fig. 6 Centerline velocity.

results behind an ellipsoidal model are also shown. His velocity recovery was even faster, since his axis ratio was 6 compared with 4 for the present model.

The blunt base shown with a dashed line is accompanied by a large recirculation region and high reverse-flow velocity. However, it is interesting to note that once past the realignment point, the centerline velocity increases so quickly that before it reaches $X/R=4.0$ the velocity defect is already even smaller than that of the flow behind the ellipsoidal bases. Apparently, the more vigorous turbulent mixing behind a bluff base helps to regain the momentum more rapidly. The maximum turbulence level behind a blunt base reaches over 20%, whereas the ellipsoidal base has a maximum level of less than 6% in its wake. Chevray's[12] data indicate that even at 10 radii downstream, the centerline velocity is only about 70% of the freestream value, and it takes over 300 radii to reach 90%.

The static pressure distribution through the near-wake shear layer is shown in Fig. 7 for various axial locations. As can be observed from the positive scale for C_p, the static pressure in the near-wake is greater than the freestream pressure approaching the base. At $X/R=0.0$, a strong radial pressure gradient can be observed. The direction of the radial gradient is reversed compared to the radial gradient in the boundary layer upstream of separation. The pressure near the base is quite high compared to the reference pressure with a corresponding velocity defect. At $X/R=1.0$, the pressure is lowered near the axis, while the freestream value slightly increases with an accompanying overall velocity drop. As the flow moves further downstream a favorable pressure gradient in the axial direction begins once more, while the gradient in the radial direction diminishes.

Figure 8 shows the stagnation pressure variation through the near-wake. In the shear layer, as expected, the stagnation pressure recovers as the velocity defect becomes smaller, although the recovery is rather slow. The profile at $X/R=0.0$ involves some error near the axis due to the large probe size relative to the very small separation region. The actual value at the centerline should be about 0.17 according to the surface tap reading that would be more reliable. The dashed portion of the curve indicates an estimate of the stagnation pressure through the separation bubble.

Velocity profiles for the near-wake obtained with the hot-wire anemometer are shown in Fig. 9. Again estimated corrections have been shown by dashed lines for the region near the separation bubble. These corrections are necessary because hot-wires have inherent problems measuring small velocities as would be found in the recirculation region.[13] From the velocity profiles, it can be seen that the maximum shear stress is much lower than for blunt base flows and it occurs between $Y/R=0.3$ and 0.4. For blunt base flows, McErlean and Przirembel[9] found the maximum shear stress at $Y/R=0.4$-0.9. Looking at the results from an alternative viewpoint, the maximum shear stress in both flowfields occurs at approximately the separation radius throughout the near- and far-wakes.

The far-wake mean velocity profiles were reduced to similarity form by transforming the coordinates such that the

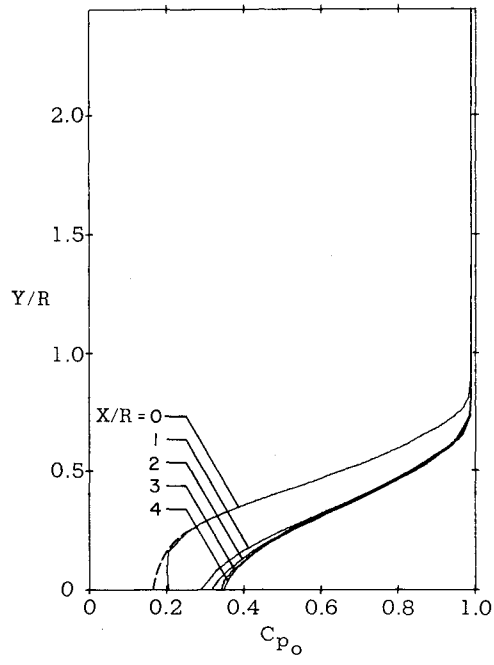

Fig. 8 Stagnation pressure profiles in near-wake.

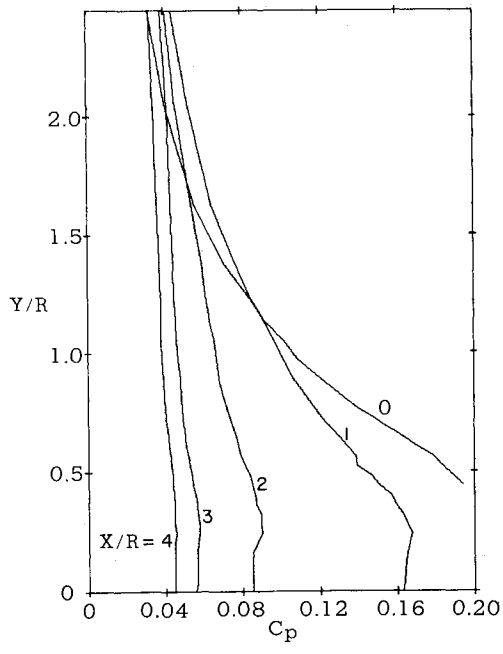

Fig. 7 Static pressure profiles in near-wake.

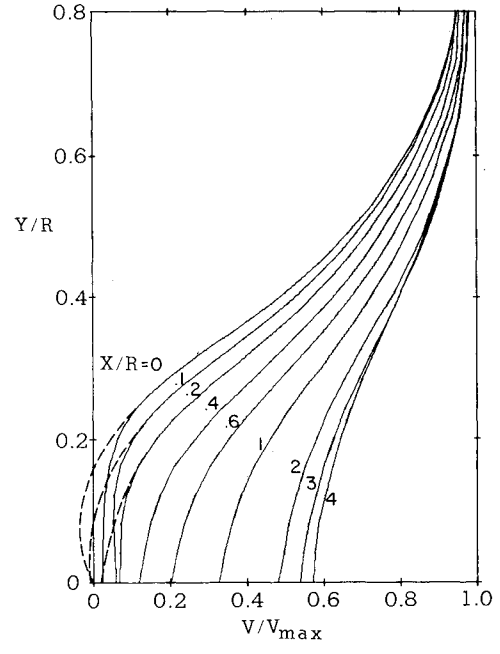

Fig. 9 Velocity profiles in near-wake.

velocity scale became $V_d/V_{d_{max}}$ and the Y scale became Y/Y_b, where

V_d = velocity defect, $= V_{max} - V$

$V_{d_{max}}$ = maximum velocity defect (at centerline)

$Y_b = Y$ where $V_d = \frac{1}{2} V_{d_{max}}$

The results are extremely consistent as plotted in Fig. 10. It can be noted that at $X/R = 0.4$, the profile has already reached almost complete similarity. This is in contrast to Chevray's[12] result of $X/R = 6$-12 and more so to Carmody's[14] result of $X/R = 30$ for the beginning of the similarity region behind a disk.

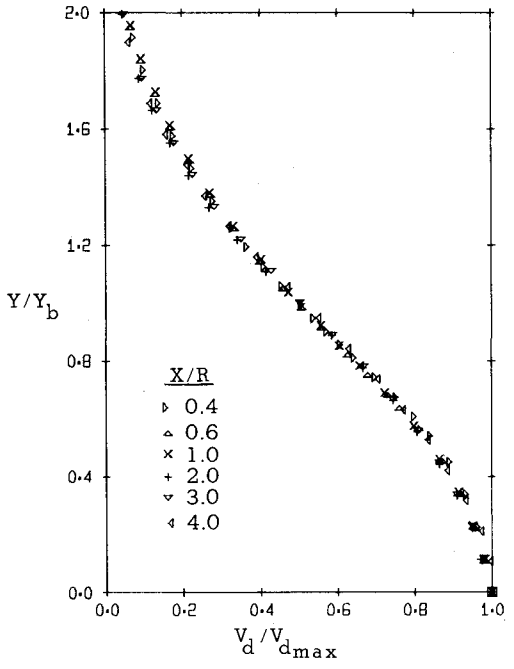

Fig. 10 Wake similarity profile.

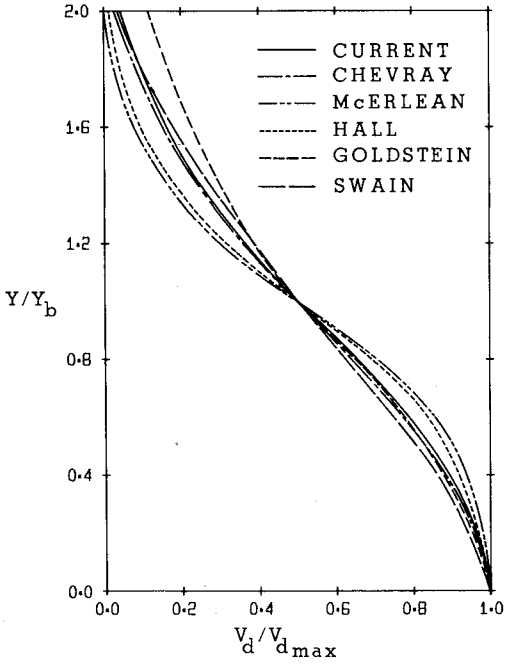

Fig. 11 Comparison of wake similarity.

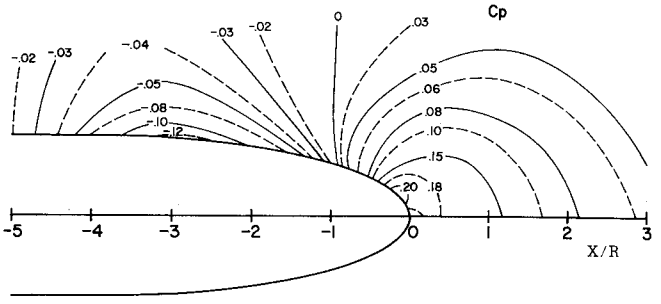

Fig. 12 Static pressure map.

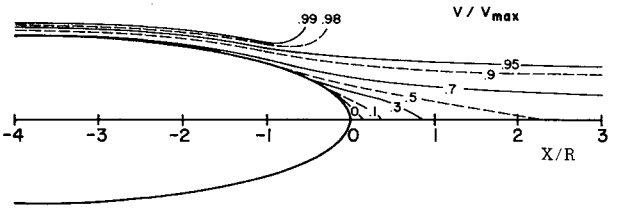

Fig. 13 Mean velocity map.

The resulting similarity profile was also compared to other researchers' results in Fig. 11. The results of McErlean and Przirembel,[9] as well as those of Hall and Hislop,[15] are based on experimental data from the blunt base. Theoretical values obtained by Swain[16] and Goldstein[17] are also included. As expected, the best agreement was obtained with the experimental results of Chevray.[12]

Comprehensive maps of the entire static pressure and velocity fields around the ellipsoidal afterbody are presented in Figs. 12 and 13, respectively. The pressure map shows lines of constant static pressure coefficient, while the velocity map plots lines of equal velocity. In contrast to blunt base flows[8,9] which have a negative base pressure coefficient, the curved afterbody has a positive coefficient. In addition, the blunt base has its lowest pressure just prior to the rear stagnation point and its highest pressure just downstream, whereas the current flow contains a relatively constant pressure around the realignment point. This is due to the wall curvature which produces a remarkably high pressure recovery. In other words, the wall curvature dominates the flow to produce a profound change in the pressure drag, while the separation and realignment processes have only a small influence.

The velocity map shows that the boundary-layer growth tends to be impeded, and even reversed, as the flow approaches the curved portion of the afterbody. As the local radius of curvature decreases, the boundary-layer thickness starts to increase again and finally jumps up as the separation line is approached. However, only the very outer region of the boundary layer ($V/V_{max} > 0.98$) was affected. The inner portion, even though the distance to the wall is still increasing, actually moves closer to the axis. Near the base, the freestream velocity may fluctuate about $\pm 1.0\%$, making the determination of $V/V_{max} = 0.98$-0.99 difficult. However, there is a definite tendency for the profile to spread rapidly in this area. After that the width of the profile decreases slightly and soon reaches an almost constant value as the far-wake is approached.

Conclusions

The turbulent near-wake of a semiellipsoidal afterbody has been investigated experimentally and the following conclusions may be drawn from the data:

1) The separation point was located at $X/R = -0.38$, while the rear stagnation point was found at $X/R = 0.2$. The

separation bubble had a length 1.34 times the model radius at separation.

2) Centerline velocity recovery for the ellipsoidal base is slower than that of a blunt base.

3) Far-wake similarity is attained as early as $X/R = 0.4$.

4) The near-wake of the ellipsoidal base had a maximum turbulence level of about 6% compared to 20% for blunt bases.

5) The maximum shear stress in the wake region is much lower than for blunt bases and is located at approximately the separation radius throughout the near- and far-wakes.

6) The effect of the separation and realignment processes on the overall flowfield is small for this model compared to the effects of wall curvature.

7) A complete set of mean pressure and velocity data in the near-wake has been obtained and will be useful in developing and evaluating analytical solutions for the flowfield.

References

[1]Schlichting, H., *Boundary Layer Theory*, 7th Ed., McGraw-Hill Book Co., New York, 1979.

[2]Chang, P. K., *Separation of Flow*, Pergamon Press, New York, 1970.

[3]Yi, C. H. and Przirembel, C. E. G., "Incompressible Turbulent Boundary Layer Separation from a Curved Axisymmetric Body," *Developments in Mechanics, Proceedings of the 13th Midwestern Mechanics Conference*, University of Pittsburgh, Pittsburgh, PA, Vol. 7, Aug. 1973, pp. 203-216.

[4]Presz, W. M. and Pitkin, E. T., "Flow Separation Over Axisymmetric Afterbody Models," *Journal of Aircraft*, Vol. 11, Nov. 1974, pp. 677-682.

[5]Presz, W. M. and Pitkin, E. T., "Analytical Model of Axisymmetric Afterbody Flow Separation," *Journal of Aircraft*, Vol. 13, July 1976, pp. 500-505.

[6]Bradshaw, P., *Experimental Fluid Mechanics*, 2nd Ed., Pergamon Press Ltd., Oxford, 1970, pp. 82-83.

[7]Nice, G. T., Tseng, W. Y., and Moses, H. L., "Separation of Turbulent, Incompressible Flow from a Curved Backward-Facing Step," Gas Turbine Lab., Massachusetts Institute of Technology, Cambridge, MA, Rept. 87, Oct. 1966.

[8]Merz, R. A., Page, R. H., and Przirembel, C. E. G., "Subsonic Axisymmetric Near-Wake Studies," *AIAA Journal*, Vol. 16, July 1978, pp. 656-662.

[9]McErlean, D. P. and Przirembel, C. E. G., "The Turbulent Near Wake of an Axisymmetric Body at Subsonic Speeds," AIAA Paper 70-797, June 1970.

[10]Van Wagnen, R. G., "A Study of Axially-Symmetric Subsonic Base Flow," Ph.D. Thesis, Mechanical Engineering Dept., University of Washington, Seattle, WA, 1967.

[11]Przirembel, C. E. G. and Riddle, R. A., "The Effect of Mass Removal from a Subsonic Axisymmetric Near-Wake," *Developments in Mechanics, Proceedings of the 14th Midwestern Mechanics Conference*, University of Oklahoma, Norman, OK, Vol. 8, March 1975, pp. 547-562.

[12]Chevray, R., "The Turbulent Wake of a Body of Revolution," *Transactions of the ASME, Journal of Basic Engineering*, Ser. D, Vol. 90, June 1968, pp. 275-284.

[13]Simpson, R. L., "Interpreting Laser and Hot-Film Anemometer Signals in a Separating Boundary Layer," *AIAA Journal*, Vol. 14, Jan. 1976, pp. 124-126.

[14]Carmody, T., "Establishment of the Wake Behind a Disk," *Transactions of the ASME, Journal of Basic Engineering*, Ser. D, Vol. 87, Dec. 1964, pp. 867-882.

[15]Hall, A. A. and Hislop, G. S., "Velocity and Temperature Distribution in the Turbulent Wake Behind a Heated Body of Revolution," *Proceedings of the Cambridge Philosophical Society*, Vol. 34, 1938, pp. 345-350.

[16]Swain, L. M., "On the Turbulent Wake Behind a Body of Revolution," *Proceedings of the Royal Society of London*, Ser. A, Vol. 125, No. 799, Nov. 1929, pp. 647-659.

[17]Goldstein, S., *Modern Developments in Fluid Dynamics*, Vol. II, Clarendon Press, Oxford, 1938.